OATAO
Open Archive Toulouse Archive Ouverte

Open Archive Toulouse Archive Ouverte (OATAO)

OATAO is an open access repository that collects the work of Toulouse researchers and makes it freely available over the web where possible.

Narrow diameter double-wall carbon nanotubes: synthesis, electron microscopy and inelastic light scattering

R R Bacsa[1]**, E Flahaut**[1]**, Ch Laurent**[1]**, A Peigney**[1]**,**
S Aloni[2]**, P Puech**[3] **and W S Bacsa**[3]

[1] Centre Interuniversitaire de Recherche et d'Ingénierie des Matériaux, Université Paul Sabatier, 31062 Toulouse Cedex 4, France
[2] Department of Physics, University of California, Berkeley, CA 94720, USA
[3] Laboratoire Physique des Solides (UMR-CNRS), Université Paul Sabatier, 31062 Toulouse Cedex 4, France
E-mail: wolfgang.bacsa@lpst.ups-tlse.fr

Abstract. Double-wall carbon nanotubes are the molecular analogues to coaxial cables. Narrow diameter double-walled carbon nanotubes (DWNTs) have been obtained by catalytic chemical vapour deposition process with high yield and characterized by scanning and transmission electron microscopy. We examine the inelastic light scattering spectrum of mostly DWNTs with internal tubes of subnanometre diameter. We observe particularly narrow radial breathing modes corresponding to the internal tubes of diameter less than 0.7 nm of double-walled tubes. The D band is found to be strongly helicity dependent and the tangential modes in narrow diameter DWNTs are found to be often down-shifted.

Contents

1. Introduction

The electronic properties of carbon nanotubes depend on the orientation of the honeycomb lattice with respect to the tube axis (helicity). A combination of an internal metallic tube with an external insulating tube forms an interesting example of a nanowire in its simplest form. It represents the molecular analogue to a coaxial cable. A carbon nanotube can be thought of as a rolled up graphene sheet. Deviations from the properties of graphite due to changes of bond angles and hybridization are expected to be strongest in narrow diameter carbon nanotubes.

Double-walled carbon nanotubes (DWNTs) were first observed by Dai *et al* [1] who reported the presence of a small number of DWNTs along with single-walled tubes during the disproportionation of CO on alumina-supported Mo particles at 1200 °C. The presence or absence of double-walled tubes was related to the nature of the catalyst by Hafner *et al* [2]. Double-walled tubes were also observed by Laurent *et al* [3] during the decomposition of methane on iron catalysts generated *in situ* during the reduction of a solid solution of iron and aluminium oxides. In this process, a mixture of single- and double-walled tubes was obtained. Similar results were obtained for a Co catalyst, and only recently it was shown by Flahaut *et al* [4] that the addition of a Mo promoter to Co nanoparticles generated *in situ* by the selective reduction of $Mg_{1-x}Co_xO$ increased the proportion of double-walled tubes to nearly 70%. A high proportion of double-walled tubes could also be obtained by the selective removal of single-walled tubes from a mixture of the two [5]. The interesting feature in the last two results is that the diameter of the internal tube is often smaller than that of the smallest observed diameter for single-walled tubes in the sample and thus it is possible to synthesize internal tubes smaller than the diameter of the C_{60} molecule. Recently, CVD processes have been reported for the synthesis of double-walled tubes by the decomposition of alcohol and methane over $Fe–Mo/Al_2O_3$ catalyst [6, 7]. Double-walled tubes have also been obtained by filling C_{60} molecules in single-shell carbon nanotubes followed by annealing [8] or by changing the catalyst in the sublimation of graphite in an electric arc [9].

Inelastic light scattering provides a wealth of information not only about the dynamics of the atomic lattice but also on low-energy electronic excitations. It is a macroscopic probe (the laser spot size is 0.5–6 μm in diameter) and extremely sensitive to small structural changes of the atomic lattice. The spectrum depends on the energy, momentum and polarization of the incident photon. At low Raman shifts (50–450 cm^{-1}) a radial symmetric breathing mode is observed for nanotubes whose energy is inversely proportional to the diameter ($\omega \propto 1/d$) [10]. This means that, as the diameter of the tube gets smaller, the sensitivity of this mode to the diameter can become very high. Although the diameter dependence of the radial breathing mode is rather well established, the calibration factor depends on the environment of the tubes (support surface, neighbouring tubes) and ranges from 220 to 248 cm^{-1} nm^{-1} [11]. The interaction with the support surface has been reported by some authors to shift the mode energy by 10 cm^{-1} [12]. For small diameter tubes the number of helicities for a given diameter range is smaller due to the discrete honeycomb lattice. If the observed peak width is smaller than the next available diameter or helicity, it becomes possible to identify the helicity of a internal carbon nanotube. We note that in some rare cases (accidental degeneracy) the same diameter can be associated with two helicities.

We present in this paper the synthesis, structural characterization and vibrational spectra of narrow diameter DWNTs. The measured diameter distribution and statistical analysis with respect to the number of walls shows that the inner diameters of several double-walled tubes are
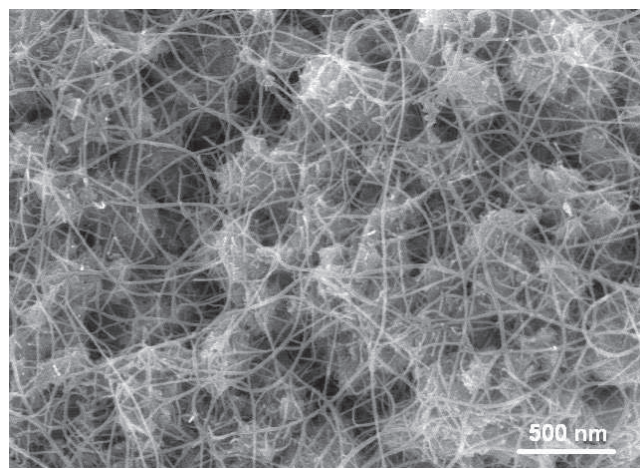
Figure 1. Scanning electron microscopy image of carbon nanotube–oxide composite formed by the selective reduction of the oxide solid solution in $CH_4 + H_2$ atmosphere at $1000\,°C$.

lower than a single-walled tube, indicating that the second wall might grow on the inside of the first wall. Furthermore, we find that the diameter of the inner tube is smaller than the diameter of the catalyst particle, which also supports the idea that the second wall grows on the inside of the first wall. Inelastic light spectra of the tubes show particularly narrow radial breathing modes, corresponding to internal tubes of diameters less than 0.7 nm, the diameter of a C_{60} molecule. Raman images of the dispersed tube samples show a large dispersion in the spectra. The D band is found to be strongly helicity dependent and the tangential modes in narrow diameter DWNTs are found to be often down-shifted.

2. Synthesis

Carbon nanotubes were prepared by passing a mixture of $H_2 + CH_4$ (18% CH_4) gas at $1000\,°C$ over nanometre sized cobalt particles generated *in situ*. The catalyst particles were produced during the selective reduction of a solid solution of $Mg_{1-x}Co_xO$ (x ranging from 0.01 to 0.1) powder. In some cases, the catalyst also contains additions of Mo (Co:Mo 3:1) [4]. In this case, the catalyst is no longer a solid solution. Dilution of CH_4 with H_2 helped to control the availability of carbon to the catalyst and the number of catalyst particles and their sizes were controlled essentially by controlling x and the grain size of the oxide solid solution [13]. The oxide solid solutions were produced by the combustion of a mixture of magnesium nitrate and cobalt nitrate in the presence of urea as a fuel. In the case of Co:Mo catalysts, urea was replaced by citric acid. Highly crystalline solid solutions of (Mg, Co)O were produced at the relatively low temperature of $550\,°C$ due to the highly exothermic nature of the combustion reaction. The evolution of large quantities of gases made the powders porous and fine grained. The highly reductive atmosphere generated during the combustion of urea maintained the Co in the Co^{2+} oxidation state which was essential to control the selectivity of the nanotube formation. After reduction, a composite containing the reduced oxide and carbon nanotubes was formed, from which the nanotubes were separated by dissolving the MgO and the unreacted cobalt metal in 1 M HCl at $25\,°C$. The chemical purity of the nanotubes was assessed by analysis of carbon by
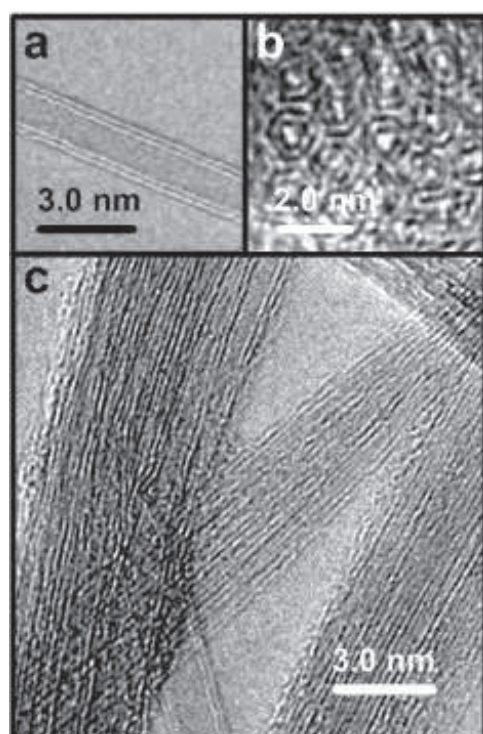
Figure 2. High resolution TEM images of carbon nanotubes after purification. (a) An individual double-walled tube; (b) end of a bundle containing double-walled tubes; (c) a larger view of the sample.

flash combustion. Poisoned cobalt particles were the principal impurity, and they were removed by boiling the nanotubes in 6 M HNO_3 for 3 h followed by oxidation in flowing air at 520 °C for 10 min [14]. This treatment reduced the cobalt content to less than 1 wt%.

3. Electron microscopy

The nanotubes were characterized by scanning and transmission electron microscopy (TEM). A scanning electron microscopy image of a carbon nanotube–oxide composite is shown in figure 1. The figure shows a network of tube bundles connected to the oxide composite. Figure 2 shows high resolution TEM images (JEOL 2011 microscope at 200 kV) of the purified nanotubes. They are principally double-walled tubes as seen in the cross section image. Only a few tubes have one or three walls. The internal diameters fall in the range 0.65–2 nm and the external diameters fall in the range 1.1–3.5 nm. We analysed the tube diameter and the number of walls in 100 tubes selected at random. Figure 3(a) shows the histogram of this analysis. We find that more than 70% of the tubes are double walled. The diameters show a wide distribution even when we use a narrow size distribution of catalyst particles. We attribute this to the formation of the second or third wall, which forms presumably on the inside or outside of the first wall. Figure 3(b) shows the internal diameter distribution of the tubes (internal diameter = external diameter for single-wall tubes) plotted against number of walls. We find that in the small diameter range 0.6–0.9 nm the majority of the tubes are double walled and that the internal diameters of several double-walled tubes are lower than the outer diameters of single-walled tubes. Comparison of
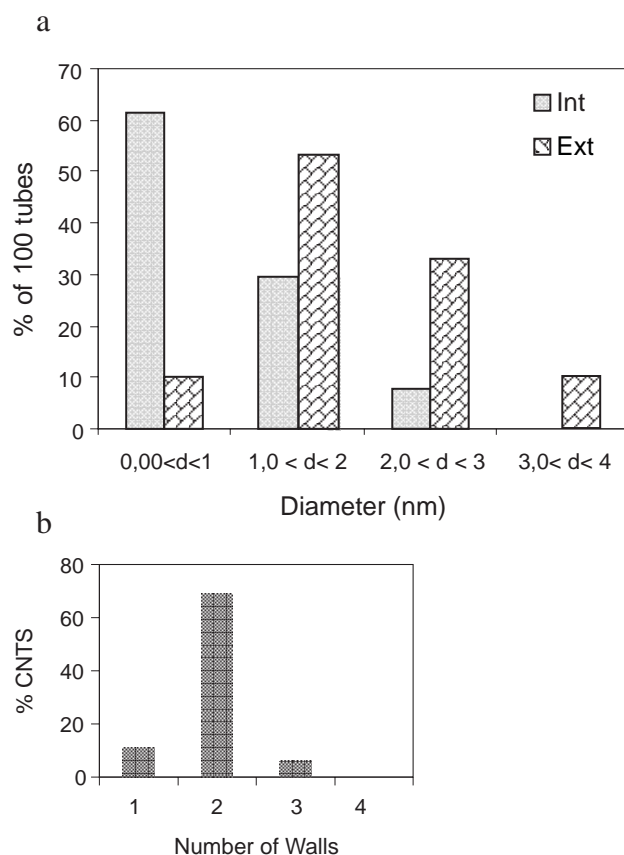
a

b

Figure 3. Histograms of (a) number of walls and (b) internal and external diameter distribution for carbon nanotube samples plotted from 100 representative high resolution TEM images.

the internal and external diameters shows that the inter-tube spacing is not constant and varies between 0.33 and 0.39 nm. In most cases it is larger than the inter-planar spacing of graphite. No amorphous or disordered carbon was seen. Although carbon nanotubes can be grown with fairly narrow diameter range their exact diameter or helicity varies from tube to tube.

4. Inelastic light scattering

We recorded Raman spectra (DILOR XY micro-Raman spectrometer) using an argon or krypton ion laser and a photon flux of less than 10 W cm^{-2}. The polarization was set parallel to the higher transmission characteristics of the spectrometer. The nanotubes were dispersed on a silicon oxide surface using a diluted solution. To enhance the Raman signal we used a bilayer substrate [15]. To explore the distribution of the heterogeneous tubes we recorded spectra along a line of the sample every micrometre. Figure 4 shows the composed Raman image which shows the Raman spectra in the radial breathing mode region as a function of the displacement on the sample surface. The Raman image shows the large dispersion of the tube diameter. All the peaks with Raman shifts of more than 220–240 cm^{-1} correspond to tubes with diameters smaller than one nanometre. The breathing modes of tubes with a neighbouring helicity in this energy range
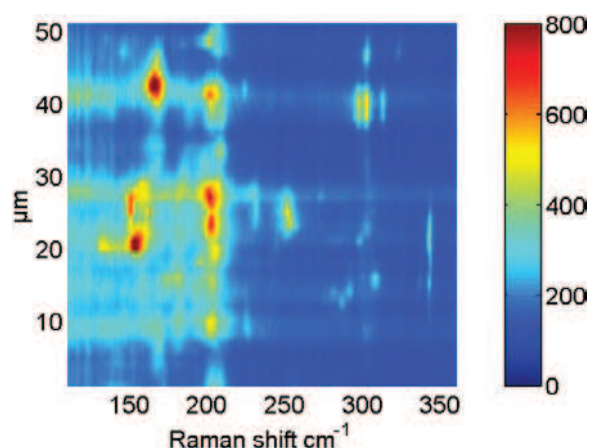
Figure 4. Raman image recorded at 488 nm consisting of 50 Raman spectra recorded in steps of 1 micrometre along a straight line.

are separated by more than the typical peak width (4 cm^{-1}). This high sensitivity of the radial mode can in principle be used to assign the helicity of the internal tubes. The assignment of the helicity depends on the scaling factor, which depends on factors such as tube environment and surface interaction. A statistical analysis of a large number of spectra on tubes placed in an equivalent environment could in principle solve this issue but is difficult to realize. Single-shell carbon nanotubes with less than one nanometre diameter are not frequent in our sample (figure 3). Spectral signatures of smaller diameter tubes are therefore attributed to internal tubes of double-walled tubes. By analysing the positions of the peaks below and above 220 cm^{-1} we can find several pairs of peaks which can be attributed to double-walled tubes. We come to the same conclusion as in the TEM image analysis: the inter-tube distance is tentatively larger than what is found for the interlayer distance in graphite. We observe that the recorded Raman peaks of the breathing mode of the tubes are very narrow and limited by the resolution of the spectrometer. Raman peaks of solids are broader by a factor of 5–15. This indicates that the phonon mean free path is very long in carbon nanotubes either due to the small number of defects or inefficient decay of the radial breathing mode due to the tubular symmetry [16]. Recent model calculations have shown that the coupling of the walls in DWNTs increases with tube diameter due to the smaller mass ratio of the two tubes [17].

The in-plane optical modes of single-wall carbon nanotubes are close to the optical mode of graphite at 1582 cm^{-1} and they are shifted to higher values. This has been explained in the past by Brillouin zone folding of the optical phonon branch. However, recent symmetry analysis of the tangential modes indicates that the observed scattering is of different origin and has been explained by double-resonant scattering which depends on the electronic band structure of the tube [18]. The often observed double peak for nanotubes is then assigned to two optical phonons with A$_1$ symmetry at the Brillouin zone centre. The same scattering has also been explained by first order scattering under resonance conditions [19]. We find that double-shell carbon nanotubes have often a down-shifted in-plane mode. The double-resonance condition depends on the electron band structure of the tube which depends on helicity. The difference observed for DWNTs can then be attributed to differences of the electron structure due to coupling of the inner and outer tubes. Recent *ab initio* calulations [20] show that the G band can be down-shifted substantially for certain DWNTs.
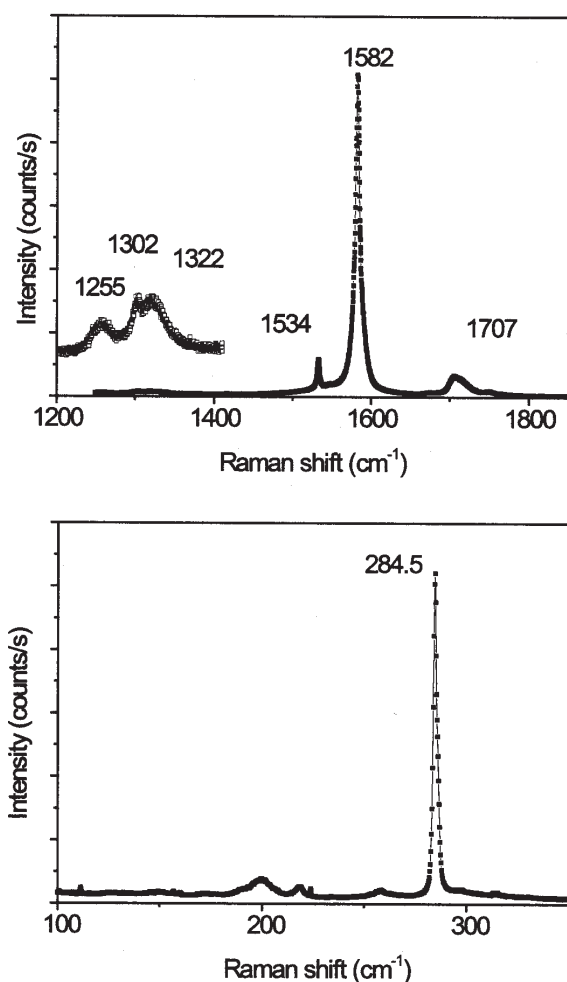
Figure 5. Raman spectra (488 nm) of radial and tangential mode energy range. One radial breathing mode is observed (284.5 cm^{-1}) which corresponds to a tube diameter 0.8 nm. The corresponding D mode is absent and the G mode is down-shifted.

Most graphitic materials show a strong band at 1350 cm^{-1} (D-band) which has been assigned to the same defect induced double-resonant Raman scattering process and is also observed for carbon nanotubes [21]. Experimental evidence of the D-band dependence on helicity has been reported in single-wall carbon nanotubes [22]. Since the electronic band structure of carbon nanotubes depends on helicity it has been pointed out [21] that the double-resonance condition must also depend on helicity. This implies that, in the case where the double resonance condition is not fulfilled for a given helicity, the D band should not appear. Although the intensity of the D band depends the number of defects or quality of the graphite structure, even tubes of high quality as verified by high resolution electron transmission microscopy show strong and mostly narrow D bands. The D-band intensity is also influenced by the singularities of the one-dimensional electronic band-structure [23].

We show in figure 5 one spectrum of a carbon nanotube sample where we observe no first order D band. Figure 5 shows in addition a spectrum in the D-band region where the intensity

has been multiplied by a factor of 20. The remaining spectral band in this region is attributed to second order scattering and has two broad contributions and a third narrower band [24]. Since the band due to the in-plane optical modes has a similar line shape compared to other spectra which have strong D bands we attribute the absence of the D band in figure 5 to the helicity dependent defect-induced double-resonance condition.

Figure 5 shows a strongly down-shifted peak at 1534 cm^{-1} possibly related to a transverse in-plane optical mode. The peak position is highly unusual and needs further investigation. The asymmetric band at 1707 cm^{-1} has also been observed in spectra from single-shell carbon nanotubes and has been attributed to combinational scattering of the tangential and radial optical modes or to defect induced double-resonant Raman process [25]. The lower part of figure 5 shows the low energy range with radial breathing mode of the spectrum on top. The intense peak at 284.5 cm^{-1} indicates that the incident light is in resonance with a tube in the 0.8 nm diameter range. The background signal has a complicated structure which indicates that scattering from different origins contributes to the spectrum, such as other radial modes and second order and defect-induced scattering.

5. Conclusion

We have described the synthesis of narrow diameter DWNTs. Scanning and TEM show that the double-walled tubes can be grown with high yield and within a fairly narrow diameter range. Inelastic light scattering shows that the tubes have a wide distribution of helicities and also shows the importance of the environment to the tube properties. The D band is found to be absent for some tubes consistent with predicted sensitivity of this band to helicity. A systematic down-shift of the G band and additional spectral signatures indicates the importance of the coupling of the two walls to the electronic properties of DWNTs.

References

[1] Dai H, Rinzler A, Nikolaev P, Thess A, Colbert D and Smalley R 1996 *Chem. Phys. Lett.* **260** 471
[2] Hafner J, Bronikowski M, Azamian B, Nikolaev P, Rinzler A, Colbert D, Smith K and Smalley R 1998 *Chem. Phys. Lett.* **296** 195–202
[3] Peigney A, Laurent Ch, Dobigeon F and Rousset A 1997 *J. Mater. Res.* **12** 613
[4] Flahaut E, Bacsa R, Peigney A and Laurent Ch 2003 *Chem. Commun.* 1442–3
    Flahaut E, Peigney A, Laurent Ch and Rousset A 2000 *J. Mater. Chem.* **10** 249–52
[5] Bacsa R, Peigney A, Laurent Ch, Puech P and Bacsa W 2002 *Phys. Rev.* B **65** R161404
[6] Wei J, Ci L, Jiang B, Li Y, Zhang X, Zhu H, Xu C and Wu D 2003 *J. Mater. Chem.* **13** 1340
[7] Lyu S, Lee T, Yang C and Lee C 2003 *Chem. Commun.* 1404
[8] Bandow S, Takizawa T, Hirahara K, Yudasaka M and Iijima S 2001 *Chem. Phys. Lett.* **337** 48
[9] Saito Y, Nakahira T and Uemura S 2003 *J. Phys. Chem.* B **107** 931
[10] Saito R, Dresselhaus G and Dresselhaus M 1998 *Physical Properties of Carbon Nanotubes* (London: Imperial College Press)
[11] Bandow S, Asaka S, Saito Y, Rao A, Grigorian L, Richter E and Eklund P 1998 *Phys. Rev. Lett.* **3779** 80

Bandow S, Chen G, Sumanasekera G, Gupta R, Yudasaka M, Iijima S and Ecklund P C 2002 *Phys. Rev.* B **66** 075416

Jorio A, Saito R, Hafner J H, Lieber C M, Hunter M, McClure T, Dresselhaus G and Dresselhaus M S 2001 *Phys. Rev. Lett.* **86** 1118–21

[12] Benoit J, Buisson J P, Chauvet O, Godon C and Lefrant S 2002 *Phys. Rev.* B **66** 073417

[13] Bacsa R, Laurent Ch, Peigney A, Vaugien T, Flahaut E, Bacsa W and Rousset A 2002 *J. Am. Ceram. Soc.* **85** 2666

[14] Nagasawa S, Yudasaka M, Hirahara K, Ichihashi T and Iijima S 2000 *Chem. Phys. Lett.* **328** 374–80

[15] Bacsa W and Lannin J 1992 *Appl. Phys. Lett.* **61** 19

[16] Pfeiffer R, Kuzmany H, Kramberger Ch, Schaman Ch, Pichler T, Kataura H, Achiba Y, Kürti J and Zólyomi V 2003 *Phys. Rev. Lett.* **90** 225501

[17] Povov V N and Henrard L 2002 *Phys. Rev.* B **65** 235415

[18] Reich S and Thomsen C 2000 *Phys. Rev.* B **62** 4273

Maultzsch J, Reich S and Thomsen C 2002 *Phys. Rev.* B **65** 233402

[19] Jorio A *et al* 2003 *Phys. Rev. Lett.* **90** 107403

Dubay O *et al* 2002 *Phys. Rev. Lett.* **88** 235506

[20] Maultzsch J, Reich S, Ordejon P, Bacsa R, Bacsa W, Dobardzic E, Damnjanovic M and Thomsen C 2003 Physics and chemistry of fullerenes and derivatives *Proc. Int. Winterschool on Electronic Properties of Novel Materials* vol 685 (Singapore: World Scientific) at press

[21] Maultzsch J, Reich S and Thomsen C 2002 *Phys. Rev.* B **64** 121407(R)

Maultzsch J *et al* 2003 *Phys. Rev. Lett.* **91** 087402

[22] Souza Filho A G, Jorio A, Dresselhaus G, Dresselhaus M S, Saito R, Swan A K, Ünlü M S, Goldberg B B, Hafner J H, Lieber C M and Pimenta M A 2002 *Phys. Rev.* B **65** 035404

[23] Kurti J, Zolyomi V, Gruneis A and Kuzmany H 2002 *Phys. Rev.* B **65** 165433

[24] Zolyomi V, Kurti J, Gruneis A and Kuzmany H 2003 *Phys. Rev. Lett.* **90** 157401

[25] Brar V W, Samsonidze Ge G, Dresselhaus M S, Dresselhaus G, Saito R, Swan A K, Ünlü M S, Goldberg B B, Souza Filho A G and Jorio A 2002 *Phys. Rev.* B **66** 155418